

Problem 10.52. Consider that a cross section varies with frequency ν as a power law, $\sigma = k\nu^\alpha$, where k and α are constants. Demonstrate that a plot of $\log \sigma$ vs. $\log \nu$ will yield a straight line. How is the slope of the straight line related to the given parameters? What is the slope of the long straight-line segment of Fig. 7a? [Ans. slope $\approx -8/3$]

Problem 10.53. Derive the *mass* fractions as defined in (40), (41), and (42) from the *number* abundances in Table 2. Assume that essentially all the mass is in the listed elements. You will have to look up the atomic weights elsewhere, e.g. on the physics.nist.gov website. Compare your results to the values quoted in the text.

11

Spectra of electromagnetic radiation

What we learn in this chapter

The distribution with frequency of radiation from a source is called a **spectrum**. It can be plotted as an energy spectrum or as a number spectrum and as a function of either frequency or wavelength. **Conversions** from one to another are possible and useful.

Continuum spectra are without spectral lines though spectral lines may be superposed upon them. They can arise from **interactions of atoms and free electrons**, for example in the solar atmosphere. Three kinds of such spectra encountered in astronomy are **thermal bremsstrahlung** from an optically thin gas, **blackbody radiation** from an optically thick gas in thermal equilibrium, and **synchrotron radiation** from a gas of extremely energetic electrons in the presence of magnetic fields. **Antenna temperatures** used by radio astronomers are a measure of specific intensity. The total power radiated by unit area of a blackbody, σT^4 , allows one to relate approximately the **radius of a star** to its **luminosity** and **temperature**.

Spectral lines arise from atomic transitions in emitting or absorbing gases. They provide powerful **diagnostics** of the regions that form the lines. **Stars** exhibit mostly **absorption lines** while **gaseous nebulae** exhibit **emission lines**. Some of the latter are **forbidden lines** which occur only at the extremely low gas densities found in space. The **shapes of spectral lines** reveal the presence of **turbulent motions** and the effects of **collisions**, the latter providing the **local density**. The **curve of growth** of a spectral line relates the **equivalent width** to the **atomic column density** along the line of sight. The **formation of spectral lines** is quantified with the **radiation transfer equation**. Its **solution** for different conditions gives insight to the formation of both absorption and emission lines.

11.1 Introduction

The spectral distribution of electromagnetic radiation from a celestial object can reveal much about the physical processes taking place at the object. The *spectral*

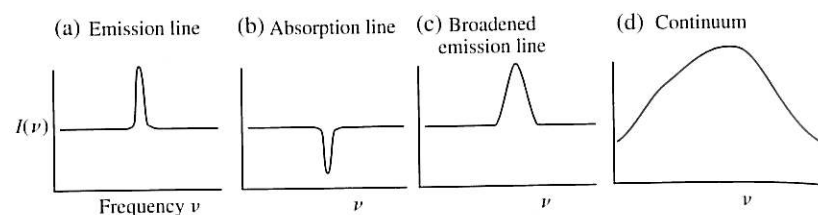


Figure 11.1. Idealized spectra of radiation: sketches of (a) line emission, (b) line absorption, (c) a broadened emission line, and (d) continuum emission. The broadening could arise from differing Doppler shifts due to differing velocities of different portions of the cloud, e.g., from rotation or turbulence.

distribution is the variation of intensity with frequency. One aspect of such studies is the study of *spectral lines*. This is an excess or deficiency of radiation at a specific frequency relative to nearby frequencies (Figs. 1a,b,c). These are called *emission lines* and *absorption lines* respectively. These lines can be quite narrow or they can be substantially broadened due, for example, to Doppler shifts arising from thermal and turbulent gas motions.

Another kind of spectral distribution is the *continuum spectrum* (Fig. 1d). This is a spectrum that varies smoothly with frequency. An emission line may or may not be superposed upon a continuum spectrum. By its very nature, an absorption line must lie upon a continuum background (Fig. 1b).

The intent of this chapter is to familiarize the reader with plotting conventions and with three commonly encountered continuum spectral shapes (optically thin thermal bremsstrahlung, synchrotron radiation and blackbody radiation). Spectral lines are formed as radiation passes through a medium of atoms. We develop the radiative transfer equation which describes this process. Its solution for various limits provides insight into the formation of spectral lines. Finally, we examine the significance of line strengths and shapes.

11.2 Plots of spectra

The manner in which astronomical spectra are presented (graphically and mathematically) is closely associated with the way we think about them. Here we discuss variants of the measurable quantities presented in Sections 8.2 and 8.4 as well as some practicalities of their use.

Energy and number spectra

The (energy) specific intensity has previously been defined (8.26) as follows:

$$I(\nu): (\text{W m}^{-2} \text{ Hz}^{-1} \text{ sr}^{-1}) \quad (\text{Energy specific intensity}) \quad (11.1)$$

This quantity is appropriate for a diffuse (resolved) celestial source, one larger in angular size than the telescope resolution. It is often rewritten in terms of other combinations of units. For example, one could choose,

$$I_p(\nu): (\text{photons s}^{-1} \text{ m}^{-2} \text{ eV}^{-1} \text{ sr}^{-1}) \quad (\text{Number specific intensity}) \quad (11.2)$$

which illustrates the two major variants: (i) the intensity is expressed as number of photons per second rather than power (energy per second), and (ii) the band is expressed in energy units (eV or J) rather than in frequency or wavelength units. A spectrum plotted with photons rather than energy in the numerator is often called a *photon spectrum* or a *number spectrum* in contrast to an *energy spectrum*. Note that the quantity “photons” is a dimensionless number,

$$(\text{photons s}^{-1} \text{ m}^{-2} \text{ Hz}^{-1} \text{ sr}^{-1}) \equiv (\text{s}^{-1} \text{ m}^{-2} \text{ Hz}^{-1} \text{ sr}^{-1}) \quad (11.3)$$

The choice between energy and photon spectra is quite arbitrary. The information content is the same in either case because at any frequency ν , the energy E of a photon is known to be

$$E = h\nu \quad (\text{J; photon energy}) \quad (11.4)$$

where $h = 6.63 \times 10^{-34} \text{ J s}$. The units of Hz are inverse seconds (s^{-1}) so the units balance.

The *number specific intensity* is converted to *energy specific intensity* simply by multiplying the number of photons in a narrow energy band $I_p d\nu$ by the energy, $E = h\nu$, of each photon in that band,

$$I(\nu) d\nu = h\nu I_p(\nu) d\nu \\ I = h\nu I_p \quad (11.5)$$

In this conversion, one must use self-consistent units, for example $h\nu$ in joules and I and I_p in the SI units of (1) and (3).

If the data represent the spectrum of a *point* (unresolved) source, the *spectral flux density* S describes the radiation. In energy units,

$$S(\nu): (\text{W m}^{-2} \text{ Hz}^{-1}) \quad (\text{Energy spectral flux density}) \quad (11.6)$$

or in terms of photons,

$$S_p(\nu): (\text{s}^{-1} \text{ m}^{-2} \text{ Hz}^{-1}) \quad (\text{Number spectral flux density}) \quad (11.7)$$

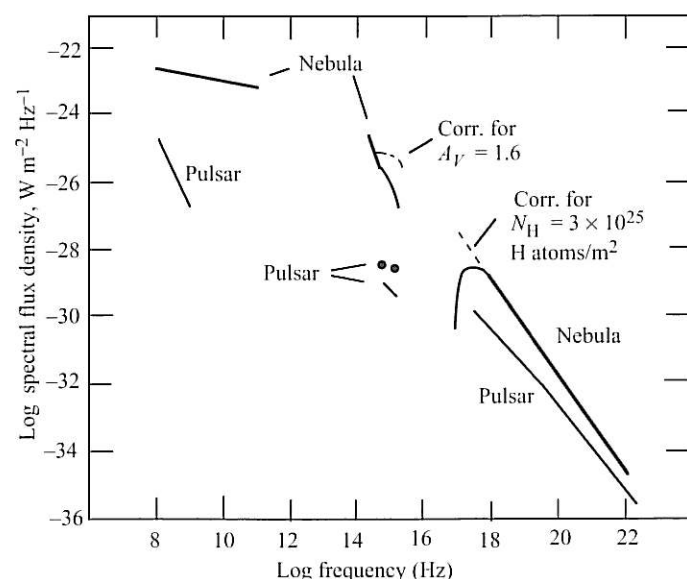


Figure 11.2. Spectrum of the Crab nebula and Crab pulsar from radio through gamma-ray frequencies. The log of the energy spectral flux density is plotted vs. log frequency. The straight-line segments are power-law spectra typical of the synchrotron emission process. The dashed lines show the spectrum that would be observed in the absence of interstellar dust and atoms. The time-average pulsar fluxes are shown as lines; typical peak fluxes of pulses are shown at two frequencies in the optical (dots). [Courtesy G. Fazio]

An example is the spectrum of the Crab nebula (Fig. 2). The Crab is not really a point source; it is a nebula several arcminutes in angular extent. However, if the instrument beam encompasses the entire source, it appears as an unresolved point source. Stated otherwise, the flux plotted is the specific intensity integrated over the angular extent of the nebula.

Astronomers tend to choose units that yield numbers close to unity because it is easier to say them. Since radio sources are many orders of magnitude less intense than the SI unit of spectral flux density ($\text{W m}^{-2} \text{Hz}^{-1}$), radio astronomers found it convenient to define a *jansky*, abbreviated as Jy,

$$1 \text{ Jy} \equiv 10^{-26} \text{ W m}^{-2} \text{Hz}^{-1} \quad (11.8)$$

The jansky was named after Karl Jansky, the discoverer of celestial radio waves (in 1932). This unit is used in Table 8.2.

Spectral reference band

Radio astronomers usually work in frequency units; optical and infrared astronomers think and work in terms of wavelength; while x-ray and gamma-ray

astronomers typically use energy units of keV or MeV. Therefore one often sees the intensity or flux quoted with respect to (per unit) wavelength λ or energy E rather than frequency ν .

Frequency and wavelength

The conversion of the specific intensity between the frequency and wavelength units was quoted in (8.43). We now derive this conversion, but we do it for the flux density S ($\text{W m}^{-2} \text{Hz}^{-1}$; frequency units). The flux density in wavelength units S_λ is power per unit area per unit wavelength interval:

$$S_\lambda: (\text{W m}^{-2} \Delta\lambda^{-1}) \text{ or } (\text{W m}^{-2} \text{m}^{-1}) \text{ or simply } (\text{W/m}^3) \quad (11.9)$$

The spectral flux density S in our usual frequency units may be written with subscript ν to distinguish it from S_λ ,

$$S(\nu) \equiv S_\nu \quad (\text{W m}^{-2} \text{Hz}^{-1}) \quad (11.10)$$

The energy flux \mathcal{F} (W m^{-2}) in a given band ν_1 to ν_2 (or the corresponding λ_1 to λ_2) must be independent of the manner in which it is expressed, giving

$$\mathcal{F} = \int_{\nu_1}^{\nu_2} S_\nu d\nu = - \int_{\lambda_1}^{\lambda_2} S_\lambda d\lambda \quad (\text{W/m}^2) \quad (11.11)$$

The minus sign is necessary if both S_ν and S_λ are to be positive quantities. (Convince yourself of this; note that $\lambda_2 < \lambda_1$ if $\nu_2 > \nu_1$.) This equality (11) is valid over any arbitrary band pass, that is, for any arbitrary interval ν_1, ν_2 (and the corresponding interval λ_1, λ_2). The only way this could be true is if the equality also holds for the integrands in (11),

$$S_\nu d\nu = -S_\lambda d\lambda \quad (11.12)$$

The frequency and wavelength in a vacuum are related as

$$\lambda = c/\nu \quad (11.13)$$

which yields the relation between the differential intervals $d\lambda$ and $d\nu$, by differentiation,

$$d\lambda/d\nu = -c/\nu^2 \quad (11.14)$$

Substitute into (12),

$$S_\nu = -S_\lambda(d\lambda/d\nu) = S_\lambda(c/\nu^2) = S_\lambda(\lambda^2/c) \quad (11.15)$$

where (13) was invoked again.

This is the desired conversion from S_λ to S_ν . It may be restated with our convention, $S \equiv S_\nu$, and with the functional arguments,

$$\Rightarrow S(\nu) = S_\lambda(\lambda) \frac{\lambda^2}{c} \quad (11.16)$$

The expression (16) properly transforms the bandwidths. The specific intensity I can be converted with the same ratio λ^2/c according to the same line of reasoning.

Frequency and energy

Energy units in the reference band in use by high-energy astronomers are usually keV or MeV rather than joules. Thus one might see S (erg cm⁻² s⁻¹ keV⁻¹). The conversion of this expression to our standard SI units S (W m⁻² Hz⁻¹) requires only numerical multiplicative factors. The conversion of erg cm⁻² to J m⁻² is made with the factors 10⁻⁷ J/erg and 10⁴ cm²/m². The conversion of keV⁻¹ to Hz⁻¹ requires the conversion factor 1/(1.6 × 10⁻¹⁶) keV/J and then the expression $E = h\nu$ which provides the conversion factor $h = 6.63 \times 10^{-34}$ J/Hz (Section 2.3). The conversion requires multiplication by the product of these four factors, or 4.14 × 10⁻²¹.

X-ray astronomers sometimes use units of I (keV s⁻¹ cm⁻² keV⁻¹ sr⁻¹). The two keVs may seem confusing, but remember that the energy term in the numerator refers to the accumulated energy and that in the denominator to the width of the energy band in which the data are being accumulated. This awareness makes straightforward the various conversions between these units.

Spectral bin widths

Data may be taken with various frequency resolutions. A high resolution (narrow bandwidth) allows one to detect and study narrow spectral lines. Since a number must be stored or telemetered for each of the many narrow spectral bands, a high resolution can require a lot of data storage space (or telemetry from a space vehicle) if the overall bandwidth is large. If, in addition, high time resolution is required, the spectral numbers must be stored for every time interval. The required data storage can be huge.

The observation time required for a spectral measurement must be such that sufficient signal or statistics are obtained in each narrow spectral or time band (often called *channel* or *bin*). For example, $N = 100$ counts (photons) must be accumulated in each channel if each is to yield a 10% uncertainty in the measured value. (See Section 6.5; we assume here negligible background.) If the 2.0 to 12.0 keV band is divided into 10 channels of 1-keV width and if the accumulation rate is uniform across the channels, a total of 1000 counts must be accumulated. Improved energy resolution of 0.01 keV, again with 10% precision, requires 1000

channels accumulating a total of 10⁵ counts. The observation time would be 100 times longer than that for the 10-channel case.

Thus, measurements with high spectral resolution carry a high price and must be used only when needed, such as for the detailed measurement of a specific spectral line. If only the broad spectral shape is desired, as in Fig. 2, then broad frequency bins will suffice.

11.3 Continuum spectra

Important examples of continuum spectra are *blackbody radiation*, *synchrotron radiation*, and *optically thin thermal radiation*. Each has a characteristic shape on a spectral plot and each reflects particular physical conditions in the source. For example, if the specific intensity or the spectral flux density of a radio source increases with frequency, the mechanism that gives rise to the emission is most likely blackbody radiation, and if it decreases with frequency it is most likely to be synchrotron radiation. The Crab nebula spectrum is an example of a continuum source with a spectrum that extends from radio to gamma-ray energies (Fig. 2). The radiation is mostly due to synchrotron radiation.

We present an observer's view of these emission mechanisms here. We derive the spectral shapes from basic physical principles in *Astrophysics Processes* (see Preface).

Free-bound, bound-free and free-free transitions

On the atomic level, continuum spectra can arise from *free-bound* or from *bound-free* transitions of the atom. The former occurs when an electron makes a transition from an unbound (free) state to a bound state, thereby emitting a photon with the energy of the transition. Since the unbound states are a continuum of energy levels, the energies, or frequencies, of the emitted photons are not restricted to well-separated discrete levels. Thus a continuum of photon frequencies (a continuum spectrum) is observed in emission.

The *bound-free* transitions are the reverse process wherein an energetic photon is absorbed and an electron is ejected into the continuum of free states. These are the photoelectric reactions discussed in Sections 10.2 and 10.5. Since photons at any energy above the ionization energy can be so absorbed, a continuum of absorption in the photon spectrum results.

Free-free transitions occur when an electron has a near collision with an atom but never becomes bound. If the electron loses energy, a photon is emitted; if it gains energy a photon is absorbed. Again, since the energy levels are not discrete, the emitted or absorbed photons exhibit a continuum emission or absorption spectrum.

An example of the free-bound and bound-free transitions occurs in the photosphere of the sun where a *second* electron can attach itself to the hydrogen atom to form a negative *hydrogen ion* H^- . As might be expected, the second electron is very weakly bound to the atom; it takes only 0.75 eV to separate it from its parent atom. This is to be compared to the 13.6-eV binding energy of the ground state. These (second) electrons can easily be detached by visible photons, which have energies well in excess of 0.75 eV (Fig. 2.1).

Most of the light from the sun arises from these ions which are constantly being formed (free-bound) and dissociated (bound-free) in the hot photosphere. The result is a continuum spectrum, except for the absorption lines that arise from the temperature gradient in the solar photosphere (see below).

Optically thin thermal bremsstrahlung

A common mechanism for the emission of photons is *thermal bremsstrahlung* from an *optically thin plasma*. A plasma is a cloud of ionized atoms or molecules. Astrophysical plasmas will typically have a mix of elements, e.g., the solar system abundances (Table 10.2). The dominant component, hydrogen, will be ionized, for the most part, into its constituent protons and electrons. The ions and electrons are typically assumed to be in approximate *thermal equilibrium*; their speeds follow the Maxwell-Boltzmann distribution. A thermal plasma must be sufficiently hot for its components to remain ionized at least in part. The term “optically thin” means that any emitted photon is very likely to escape the cloud without being absorbed by another atom; the optical depth of the cloud is small, $\tau \ll 1$; see (10.30).

Radiation from a hot plasma

In a plasma cloud, the radiation arises when electrons are accelerated in near collisions with ions and thereby emit photons. The term “bremsstrahlung” means “braking radiation” in German. In an electron-ion near collision, the less-massive electron undergoes a large acceleration due to the mutual Coulomb force. An accelerated electric charge will always radiate away some of its energy. The radiated photons constitute the observed radiation. Bremsstrahlung gives rise to the x rays in your dentist’s x-ray tube. High-energy electrons beamed into a metal target are rapidly braked to a stop by Coulomb interactions. The deceleration results in an intense beam of x rays.

The dependence of the volume emissivity j ($W m^{-3} Hz^{-1}$) of emitted radiation upon temperature T and frequency ν may be approximately obtained in a semi-classical derivation. This derivation (not worked out here) takes into account only the free-free collisions of electrons and ions. It thus yields only a continuum spectrum. A complete solution taking into account free-bound and bound-free transitions would yield strong emission lines.

The resultant continuum spectrum is

$$j(\nu, T) \propto g(\nu, T, Z) Z^2 n_e n_i T^{-1/2} e^{-h\nu/kT} \quad (W m^{-3} Hz^{-1}) \quad (11.17)$$

where h and k are the Planck and Boltzmann constants respectively ($h = 6.63 \times 10^{-34} J s$; $k = 1.38 \times 10^{-23} J K^{-1}$), n_e and n_i are the number densities (m^{-3}) of the electrons and ions respectively, and Z is the atomic number (charge number) of the ions. The *Gaunt* factor $g(\nu, T, Z)$ is a slowly varying term (decreasing with frequency) that takes into account the quantum mechanical effects in the free-free collisions, such as *screening* by nearby electrons. In the approximation, $g = \text{constant}$, the dependence of j on frequency at a fixed temperature is a simple exponential. The exponential reflects the thermal Maxwell-Boltzmann distribution of electron speeds.

Plasma parameters determined

The quantity that one can measure from afar is the specific intensity I which is related to j according to (8.50),

$$I = \frac{1}{4\pi} \int_0^A j(r) dr \quad (\text{Specific intensity; hydrogen plasma; } (11.18)$$

$$\propto \frac{1}{4\pi} \int_0^A n^2 T^{-1/2} \exp(-h\nu/kT) dr$$

$W m^{-2} Hz^{-1} sr^{-1})$

where we assume $g = \text{constant}$ and adopt a pure hydrogen plasma, so $Z = 1$ and $n_i = n_e \equiv n$. The integration is along the line of sight through the entire depth A of the cloud; recall that the cloud is optically thin. If one further assumes that the densities and temperature are constant through the depth of the cloud,

$$I \xrightarrow{j = \text{const.}} \frac{j}{4\pi} A \quad (\text{Constant } n, T) \quad (11.19)$$

$$\propto n^2 A T^{-1/2} \exp(-h\nu/kT)$$

This function is sketched in Fig. 3 for two temperatures, $T_2 > T_1$, on linear, semilog and log-log axes. The unspecified proportionality constants in (17) are taken to be equal in the two cases; thus Fig. 3 compares the spectra of two hydrogen plasmas that have different temperatures, but which are otherwise identical.

The linear plot (Fig. 3a) shows the typical exponential decrease with increasing frequency. The higher temperature for the T_2 curve is reflected in two ways. It has less amplitude at $\nu = 0$, as a consequence of the $T^{-1/2}$ dependence, and it falls to $1/e$ of its $\nu = 0$ amplitude at a greater frequency than does the T_1 curve. The higher temperature plasma emits more high-energy photons as might be expected.

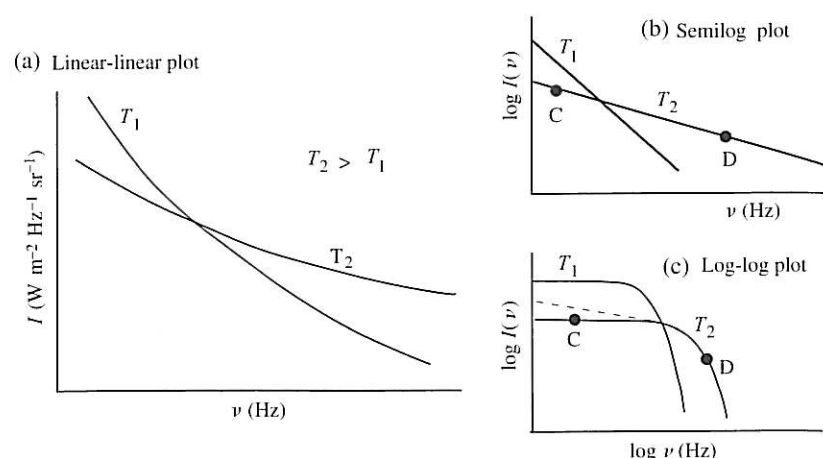


Figure 11.3. Sketches of exponential spectra on linear-linear, semilog, and log-log plots for two sources with differing temperatures, T_2 and T_1 . In each case, most of the energy is emitted at the higher frequencies. Measurements of the flux at points C and D permit one to solve for the temperature T of the plasma as well as the factor $n_e^2 \Lambda$ where n_e is the electron density and Λ is the line-of-sight thickness of the cloud. The dashed line in (c) illustrates the effect of the Gaunt factor for the T_2 curve in a realistic thermal bremsstrahlung spectrum. These plots do not show the prolific emission lines typical of a real plasma.

The semilog plot (Fig. 3b) shows the same features with the typical straight-line character of exponential functions.

The log-log plot (Fig. 3c) is interesting; it shows a flat spectrum out to a certain region where it starts to decrease rapidly. (We show the effect of a hypothetical Gaunt factor g with a dashed line.) The turnover occurs near the frequency given by $h\nu \approx kT$. At this frequency, the kinetic energy of the emitting electrons, $\sim kT$, is about equal to the energy of the individual emitted photons $h\nu$. Most of the power is emitted in this frequency region. At lower frequencies, $h\nu \ll kT$, the exponential function in (17) is approximately unity; recall that an exponential with a small argument ($x \ll 1$) may be approximated as $e^x = 1 + x \dots \approx 1.0$.

On a logarithmic abscissa, the low-frequency portion of the function near $h\nu \ll kT$ may be stretched out indefinitely toward $\nu = 0$, to 0.1 Hz, to 0.01 Hz, to 0.001 Hz, etc.; this is why it is flat. Relatively little power is included in the low-frequency regions because the bandwidths are so small. For example, the band 0.1 to 1 Hz has a bandwidth of 0.9 Hz while the band 0.001–0.01 Hz has a bandwidth of only 0.009 Hz. The power in each decade is proportional to the product of I and the bandwidth. At low frequencies, I is constant but bandwidth becomes negligibly small. This explains qualitatively our statement that most of the emitted power is at frequencies near the cutoff at $h\nu/kT \approx 1$.

Measurement of the specific intensity curve $I(\nu)$ provides direct information about both the product $n^2 \Lambda$ and the temperature T of the cloud. Consider the approximate expression for $I(\nu)$ (19), for a hydrogen cloud of constant temperature and density along the line of sight with a fixed Gaunt factor. The temperature T is obtained directly from the value of ν where I is at e^{-1} of the maximum, namely at point D in Fig. 3c; at this frequency, $h\nu/kT = 1$. The value of I at low frequencies (point C) yields the product $n^2 \Lambda T^{-1/2}$. Since T is known, we obtain $n^2 \Lambda$. The unspecified proportionality constant in (19) is a combination of well known physical and numerical constants, so absolute values of T and $n^2 \Lambda$ are obtained.

Shocks in supernova remnants, stellar coronae, H II regions

The actual spectral form for thermal bremsstrahlung is not a pure exponential. The Gaunt factor causes the flat portion of the log-log plot to decrease slowly with increasing frequency. Also the several atomic elements in cosmic plasmas lead to strong emission lines superposed on the quasi exponential continuum. A theoretical calculation (Fig. 4) of the expected radiation from a plasma of temperature 10^7 K containing “cosmic” abundances of the elements (e.g. Table 10.2) shows both of these effects.

On the semilog plot of Fig. 4, the Gaunt factor appears at low photon energies $h\nu$ as an excess above the extrapolated straight-line continuum seen at higher frequencies. This continuum decreases by a factor of about $e = 2.7$ for each increase of $h\nu$ by a factor kT as expected from (17). Note that the emission lines typically exceed the continuum in intensity by two decades, a factor of ~ 100 .

Such hot x-ray emitting plasmas are found in shock waves propagating outward from the sites of supernova explosions, for example in the supernova remnant Puppis A (Fig. 5a). Coronae in the vicinity of stars like our sun are hot plasmas of temperatures reaching 10^6 K and more. In some cases, e.g. Capella (Fig. 5b), the radiation is sufficiently hot and intense that the currently orbiting Chandra observatory can resolve its spectral lines. In both cases, the emission lines are plotted on a linear scale which dramatically illustrates how the spectral line intensities greatly exceed the continuum, in accord with Fig. 4.

Thermal bremsstrahlung emission is found in radio emitting low-temperature plasmas of emission nebulae such as H II regions of the Orion nebula (Fig. 6b). The ideal spectrum for such a source is sketched in Fig. 6a. The flat ($\alpha \approx 0$) portion is the low-frequency end of an optically thin thermal bremsstrahlung spectrum with $g = \text{constant}$ (compare to Fig. 3c).

At very, very low frequencies, plasmas become optically thick; the nebula becomes opaque to its own radiation because the number of *phase space* states the photons can occupy are limited at the low frequencies. (Phase space is six-dimensional

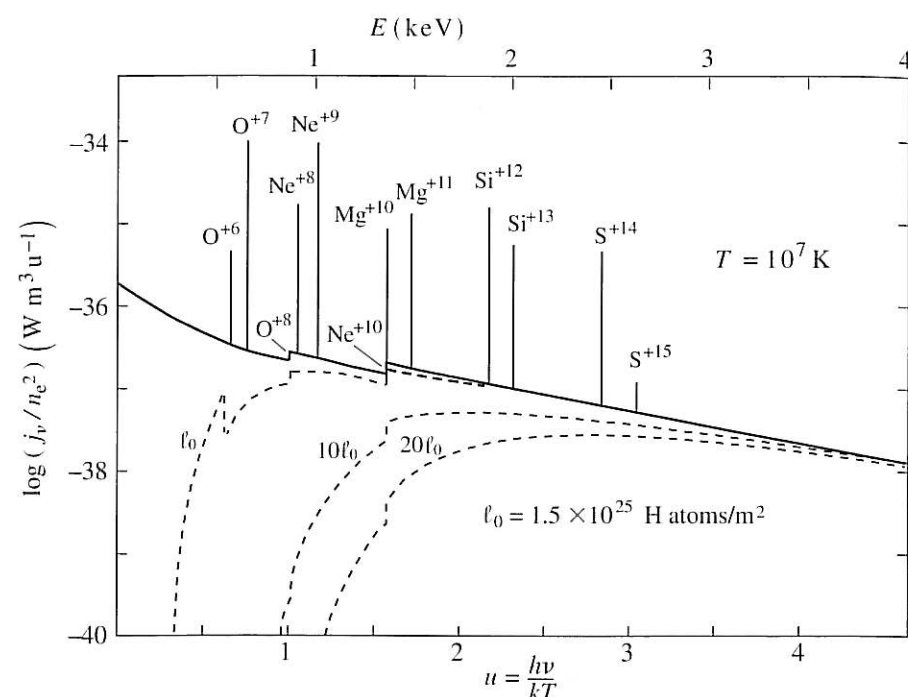


Figure 11.4. Theoretical x-ray spectrum of an optically thin plasma at $T = 10^7$ K on a semilog plot. The ordinate is the log of the volume emissivity j (17) divided by electron density squared. The abscissa is unity at the frequency where the exponential term in (17) equals e^{-1} . The various atomic levels are properly calculated, and strong emission lines are the result. The dashed lines show the effect of photoelectric absorption of x-rays by interstellar gas. [From Tucker and Gould, *ApJ* **144**, 244 (1966)]

with 3 momentum and 3 position coordinates.) The spectrum thus descends like the low-frequency part of a blackbody spectrum which is similarly constrained by available phase space states. This portion of the spectrum has the ν^2 Rayleigh–Jeans dependence (see below).

Synchrotron radiation

A mechanism that can give rise to a spectrum of very different shape is *synchrotron radiation*. This occurs when very high energy (relativistic) electrons spiral around magnetic field lines due to the $q\mathbf{v} \times \mathbf{B}$ force on an electric charge q moving with velocity \mathbf{v} in a magnetic field \mathbf{B} . The electrons emit electromagnetic radiation because the spiraling motion constitutes an acceleration, and accelerating charges emit photons. Because the charges are relativistic, the radiation is particularly intense, and it can reach to extremely high energies, even to x rays and gamma rays. It is also

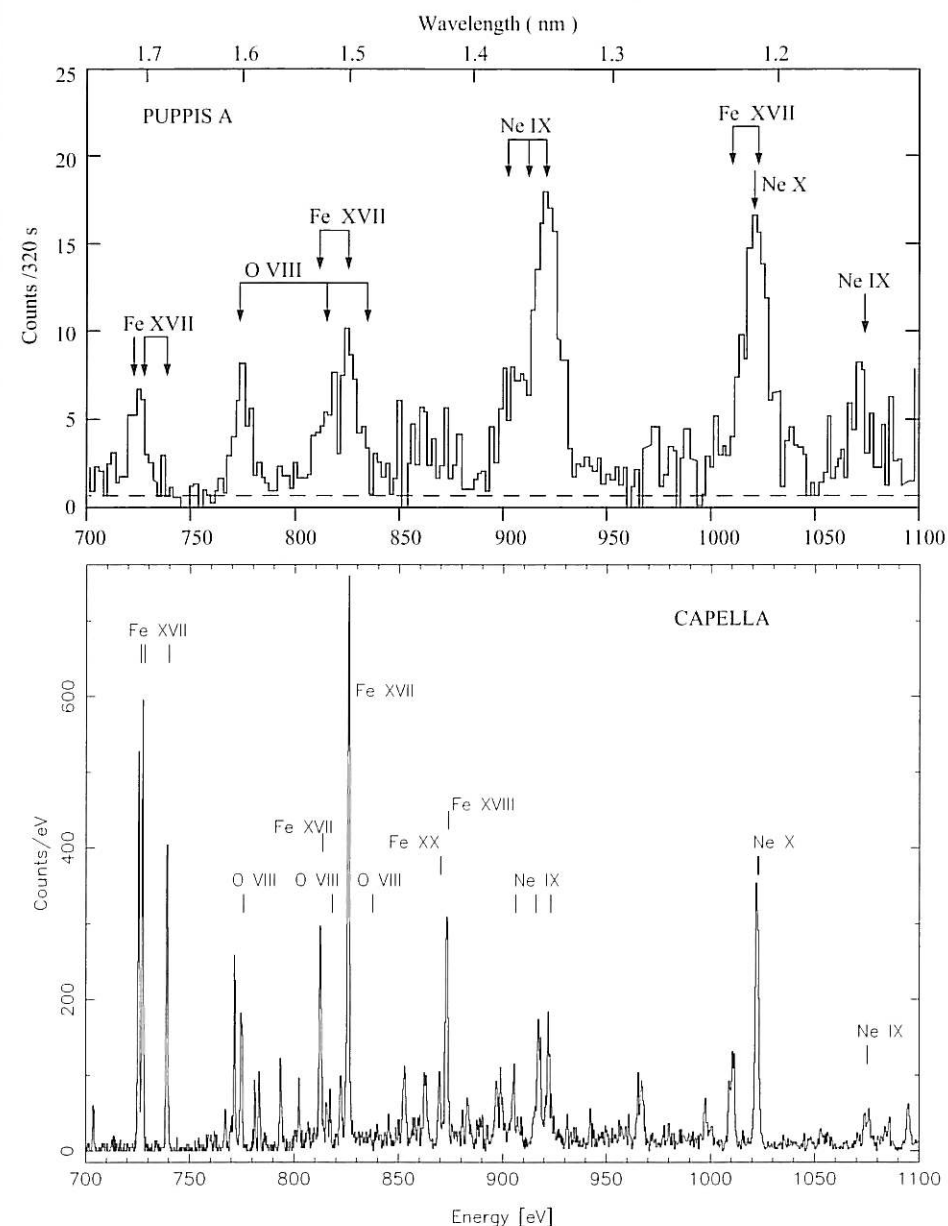


Figure 11.5. High resolution x-ray spectra of (top) the supernova remnant Puppis A from the historic Crystal Spectrometer on the Einstein observatory (launched 1978) and (bottom) the bright star Capella from the High Energy Grating Spectrometer on the Chandra observatory (launched 1999), for the same part of the spectrum. The resolution of the latter is much improved over the former. The locations of some spectral lines expected at x-ray temperatures are indicated. The relative strengths of the observed lines indicate temperatures, densities and compositions of the plasmas (a) in the shock wave that originated in the supernova explosion of Puppis A and (b) in the plasma of the active corona of Capella. [Top: adapted from Winkler *et al.*, *ApJ Lett.* **246**, L27 (1981); bottom: from C. Baluta and K. Flanagan from archival calibration data; also see Canizares *et al.*, *ApJL* **539**, L41 (2000)]

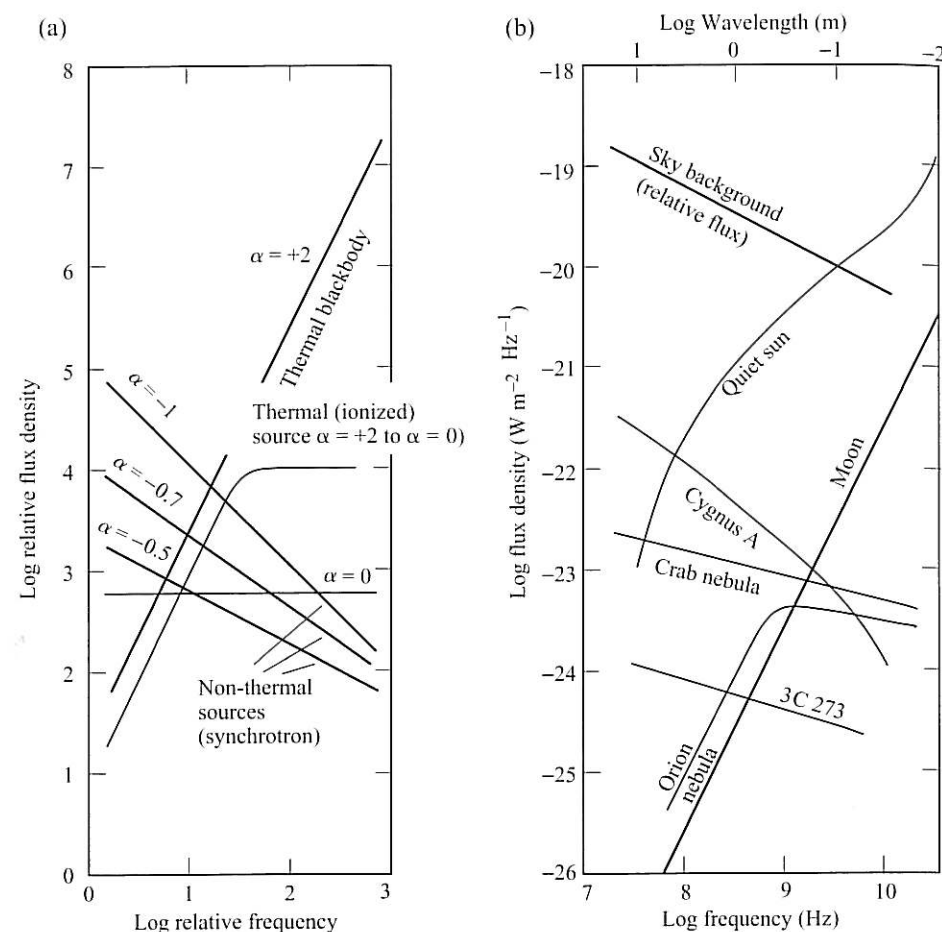


Figure 11.6. (a) Sketches of ideal radio spectra that are (i) rising (optically thick thermal, typically blackbody), (ii) falling (non-thermal, typically synchrotron radiation), and (iii) flat (optically thin thermal radiation). (b) Sketches of real radio spectra. Note that, at very low frequencies, the flat optically thin spectra become optically thick and take on the ν^2 power-law character of blackbody intensity for $h\nu \ll kT$. The sky background was measured over an unspecified solid angle. [Adapted from J. D. Kraus, *Radio Astronomy*, 2nd ed. Fig. 8-9, Cyg-Quasar Books, 1986, with permission]

beamed in the direction of travel of the radiating electron, like the headlight of an automobile. It can also exhibit polarization that reflects the large scale coherence of magnetic field directions in the source region.

The observed spectrum from a source radiating by the synchrotron process reflects primarily the distribution of energies of the radiating electrons. The energy spectrum of these electrons often has a characteristic shape, a *power law*, and this

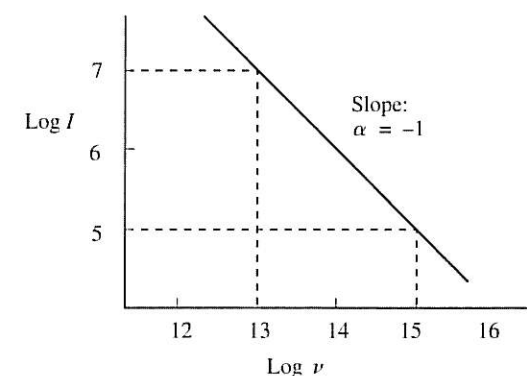


Figure 11.7. Schematic of a power-law spectrum, $I \propto \nu^\alpha$ where $\alpha = \text{constant}$. On a log-log plot, as shown here, the spectrum is a straight line with slope α .

leads to a radiated photon spectrum that is also a power law. The spectrum of the radiation can thus be represented, of course, by a power-law function,

$$I = K \nu^\alpha \quad (11.20)$$

where I is the specific intensity, K is a constant, and α is a constant exponent. In nature, power-law spectra usually decrease with frequency, in which case α is negative. Because of this, a positive *spectral index* $\beta \equiv -\alpha$ is often defined so that $I = K \nu^{-\beta}$. It is important to specify which convention you use; we use the convention (20).

A power law is most conveniently plotted in a log-log format (Fig. 7). In this format, a power law is a straight line with a slope equal to the exponent, α . This is apparent if one takes the logarithm of (20),

$$\log I = \log K + \alpha \log \nu \quad (11.21)$$

The exponent α is thus the *logarithmic slope*. From it, one can deduce the logarithmic slope of the energy spectrum of the radiating electrons.

The slope is obtained from a spectrum by using logarithmic intervals. For instance, in Fig. 7,

$$\alpha = (5 - 7)/(15 - 13) = -1 \quad (11.22)$$

The slope can be measured as a ratio of distances if the ordinate and abscissa both have the same scale factors, that is, a decade is the same distance on both axes. It is often helpful to construct log-log plots with equal scales because the slope which equals α can readily be estimated by eye.

Blackbody radiation*Spectrum*

An emitting body can be *optically thick*. The conditions are such that the photons scatter, or are absorbed and re-emitted, many times prior to being emitted from the surface. In this case one obtains a spectral shape known as the *blackbody spectrum*. The spectrum depends upon the temperature of the emitting body. Many ordinary objects emit radiation that approximates a blackbody spectrum. Objects at room temperature ($T \approx 300$ K) emit photons with a spectrum characteristic of $T \approx 300$ K (infrared radiation), and a piece of iron heated until it glows a yellow color emits at $T \approx 1100$ K. At ~ 5000 K, the color is “white hot”; which is typical of the sun. These spectra are also called optically thick thermal spectra in contrast to the optically thin thermal bremsstrahlung discussed above.

Blackbody radiation is a well defined physical quantity. It is the radiation one would find inside an evacuated cavity of a given temperature with “black” walls that absorb and re-emit radiation freely such that they are in thermal equilibrium with the radiation in the cavity. At a given frequency and temperature, the specific intensity $I(\nu, T)$ of the radiation inside the cavity is a well determined function that can be calculated from basic physics principles. It could not be explained with classical physics, but in the early years of the last century, Max Planck was able to explain it in terms of quantum mechanics.

The specific intensity for blackbody radiation, the *Planck radiation law*, in terms of the frequency ν and temperature T , is

$$\Rightarrow I(\nu, T) = \frac{2h\nu^3}{c^2} \frac{1}{e^{h\nu/kT} - 1} \quad \text{(Planck radiation law; } \text{W m}^{-2} \text{ Hz}^{-1} \text{ sr}^{-1}) \quad (11.23)$$

where h and k are the Planck and Boltzmann constants and c the speed of light.

Again this is a continuum spectrum; the ideal blackbody spectrum has no spectral lines. Also note that the amplitude at a given temperature and frequency is completely specified. There are no other parameters such as the density or charge of the atoms in the source. At a given frequency, there is no such thing as fainter or brighter blackbody radiation at a specified temperature T . The intensity is fixed by T ; blackbody radiation is blackbody radiation, period.

The expression (23) is plotted for two temperatures in Fig. 8 with linear axes and with log-log axes. The exponential temperature dependence causes the amplitude to change dramatically even for a modest change in temperature, a factor of 2 in the figure. For this reason, it is often convenient to use logarithmic axes.

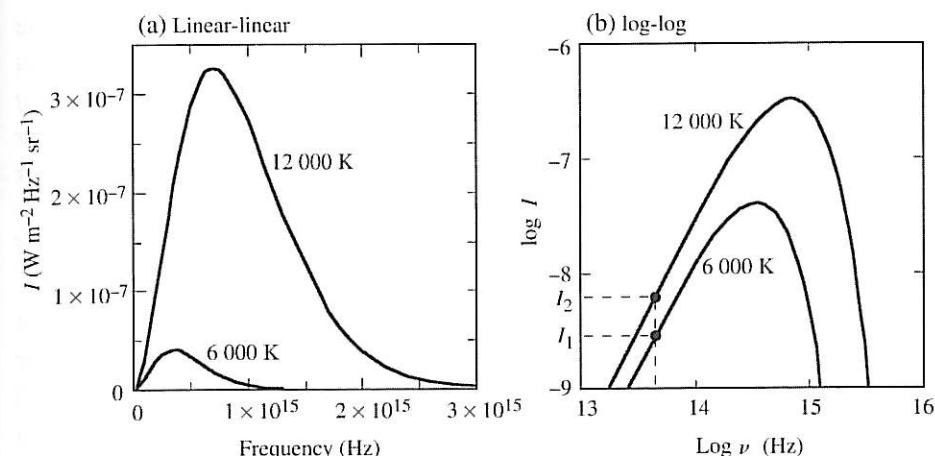


Figure 11.8. Sketches of blackbody spectra for two temperatures on both linear and log-log plots, according to (23). The temperatures differ by a factor of 2. Note the following features: the power-law behavior at low frequencies, $I \propto \nu^2 T$, the rapid decrease at high frequencies caused by the exponential term, the frequency of the maximum intensity increasing with temperature, and the rapid growth as a function of temperature. At a specified low frequency, the temperature T may be used as a shorthand for the specific intensity I , since $I \propto T$.

Radio spectra and antenna temperature

At frequencies significantly less than that of the peak frequency, the blackbody function varies linearly with the temperature and quadratically with frequency:

$$\Rightarrow I(\nu, T) \approx \frac{2\nu^2 kT}{c^2} \propto \nu^2 T \quad \text{(Rayleigh-Jeans law)} \quad (11.24)$$

This expression follows from an expansion of the exponential, $e^x = 1 + x + \dots$ for $x \ll 1$. It is called the *Rayleigh-Jeans law* (R-J law) or more appropriately, the *Rayleigh-Jeans approximation*. Note that it is a power law in frequency, $I \propto \nu^2$, so that it becomes a straight line with slope 2 on the low-frequency end of a log-log plot (Fig. 8b). It is also directly proportional to temperature T ; a factor of 2 increase in T leads to a factor of 2 increase in the specific intensity in this low-frequency portion of the spectrum.

The lowest temperature encountered in space is $T = 2.73$ K (the cosmic background radiation), and it has a peak at $\nu = 160$ GHz or at wavelength $\lambda = 1.9$ mm. This is at the extreme upper end of the radio band. In the radio portion of the electromagnetic spectrum, therefore, the blackbody spectrum for all expected temperatures is rising. It is therefore usually appropriate to invoke the low-frequency approximation, the R-J law (24), for measurements in the radio region.

Since the specific intensity is directly proportional to the temperature of the radiation in the R-J approximation, radio astronomers often report intensities as equivalent temperature $T(K)$ at some specified frequency. The phrases *antenna temperature* and *brightness temperature* are used to describe this temperature. For example, the two data points (filled circles) in Fig. 8b may be described as either the values of I_1 and I_2 in SI units or as the temperatures 6000 K and 12 000 K, respectively. Note that the same antenna temperature T represents larger values of I at higher frequencies.

Even if the object does not have a blackbody spectrum, the antenna temperature may be used to represent a measurement of I at some frequency ν . At another frequency, the antenna temperature could well have a different value. (It would be the same if the spectrum were precisely blackbody.) One converts from antenna temperature T to specific intensity I with the expression (24), or more precisely (23), where the frequency of the observation is used for ν .

Radio astronomers traditionally characterize broadband spectra as rising, falling, or flat according to the behavior of the spectral flux density as frequency increases. Figure 6a shows a variety of theoretical spectral shapes. The rising spectra all have slope $+2$ consistent with (24) and are called *thermal spectra*. The falling spectra are called *non-thermal*. These latter spectra were so named because they do not rise as does a thermal spectrum. Later, it was realized that such spectra frequently indicate synchrotron radiation. The term “non-thermal” remains appropriate because the emitters are ultra-high-energy electrons that are *not* in thermal equilibrium with their surroundings.

Real examples of radio spectra are shown in Fig. 6b. The quiet sun and the moon are largely thermal whereas the radio galaxy Cygnus A, the quasar 3C273, the Crab supernova remnant, and the sky background are all non-thermal (synchrotron radiation). The Orion nebula (an H II region of ionized plasma) exhibits an approximately flat spectrum that becomes optically thick at low frequencies.

Cosmic microwave background

A beautiful example of blackbody radiation is the remnant radiation from the early hot, dense universe. The cosmic background radiation (CMB) would have had a blackbody spectrum of temperature $T \approx 3000$ K when the cooling and expanding universe first became optically thin to this radiation. This occurred when protons and electrons combined to become neutral hydrogen. By now the radiation has cooled to $T \approx 3$ K, and is expected to still have the spectral shape of blackbody radiation.

Such radiation was discovered in 1964 by Penzias and Wilson at Bell Laboratories in New Jersey; a Nobel-prize winning discovery. Another earlier indication, in 1941, of this radiation was derived from optical spectral-line observations of starlight

absorbed by cyanogen (CN) molecules in interstellar space, but this was before the predictions of such radiation so the result received little notice. (The method of the CN detection was discussed in Section 9.4.) The 1964 discovery was a great surprise because the scientific community did not generally recognize at that time that such radiation would be a consequence of the big bang theory. In fact, its existence had been suggested in the 1940s and its temperature predicted to be ~ 5 K in a 1950 paper.

Early measurements of the CMB are shown in Fig. 9a where they are compared to a blackbody spectrum. Note that the detections at several different frequencies by several different groups verified that the spectrum rises $\propto \nu^2$ as expected for blackbody radiation, but the high frequency fall off could not be confirmed with ground-based experiments.

The galactic background (non-thermal synchrotron radiation) is also shown in Fig. 9a. One reason the thermal radiation was not discovered earlier is that the galactic background dominated the radio fluxes at lower frequencies where most measurements were made. It is only at the higher frequencies that the thermal fireball radiation exceeds the non-thermal galactic background.

The spectral shape of the CMB has been determined with great precision by the COBE satellite (Cosmic Background Explorer; launched 1989). The published spectrum (Fig. 9b) shows dramatically the agreement with a blackbody spectrum on both sides of the peak. The temperature is found, also with high precision, to be $T = 2.725 \pm 0.002$ K.

This precise agreement with a blackbody spectrum strongly supports the model of a hot early universe (big bang). The radiation is highly isotropic; it arrives from all directions with nearly the same intensity. This too is consistent with expectations; the entire universe is immersed in this radiation. Ongoing studies of minuscule fluctuations of CMB intensity (temperature) from point to point on the sky with satellites and balloons further probe the nature of the early universe.

Stars

The overall shape of the spectra of many stars approximates that of a blackbody, and blackbody formulae are often adopted to describe their energy output. Nevertheless the spectrum is substantially distorted by absorption lines and by the effect of the temperature variation with depth in the stellar atmosphere. In the spectrum of Canopus (Fig. 10a), the absorption lines are obvious deviations.

There is also severe *continuum absorption* rightward of 365 nm (3.40 eV) due to electrons in the $n = 2$ state of hydrogen being ejected into the continuum. Photons more energetic than 3.40 eV can be absorbed by the transition. In hot stellar atmospheres, sufficient numbers of atoms are found in the $n = 2$ level to make this absorption substantial.

Consider 1 m^2 of the stellar surface and let it radiate as a perfect blackbody into all directions in the upper hemisphere. Integrate the spectrum over all frequencies and all directions, taking into account the projected area, $\cos \theta$, at angle θ to obtain the total power radiated by the 1 m^2 . It turns out to be

$$\Rightarrow \mathcal{F} = \sigma T^4 \quad (\text{W m}^{-2}; \text{blackbody radiation}) \quad (11.25)$$

where σ is the *Stefan–Boltzmann constant*:

$$\sigma = \frac{2\pi^5 k^4}{15 c^2 h^3} = 5.670 \times 10^{-8} \text{ Wm}^{-2} \text{ K}^{-4} \quad (\text{Stefan–Boltzmann constant}) \quad (11.26)$$

The calculated flux (25) is that which passes in one direction through a surface immersed in a blackbody cavity. The total flux (in both directions) through the surface would be zero. The flux (25) increases rapidly with temperature. A doubling of the temperature yields a power greater by a factor of 16.

Since the spectrum from a normal star approximates that of a blackbody, one can use (25) to estimate its luminosity in terms of its surface temperature T and radius R . The surface area of the spherical star is $4\pi R^2$ and its luminosity is $L \approx 4\pi R^2 \sigma T^4$. The approximate equality indicates that the star does not emit as a perfect blackbody. In Section 9.4, we defined an *effective temperature* T_{eff} (9.13) to yield the exact relation,

$$\Rightarrow L = 4\pi R^2 \sigma T_{\text{eff}}^4 \quad (\text{W}; \text{luminosity of spherical object}) \quad (11.27)$$

The total power L radiated by a star thus varies as the fourth power of T_{eff} and the second power of its radius R .

Models of normal stars tell us that the more massive stars are both larger and hotter. In a simple model, the luminosity increases extremely fast with temperature, approximately as $L \propto T_{\text{eff}}^5$ for lower mass stars where the dominant fusion process is initiated by a proton–proton interaction, the *p–p process*. For the massive hotter stars where fusion interactions involving carbon, nitrogen and oxygen take place, the model indicates $L \propto T^{13}$. A small rise of surface temperature signifies a huge increase in the output from the thermonuclear reactions that power the star.

11.4 Spectral lines

Spectral lines provide powerful diagnostics of the conditions in the emitting region of a celestial source. Normal stars exhibit absorption lines due to decreasing temperature (with altitude) in the photosphere (Fig. 10a) while ejected gas near a star or an active corona can result in emission lines (Fig. 10b). Here we discuss the

several types of spectral lines and their measurable characteristics. In the following section, we present the physics of radiation propagation that creates the lines.

Absorption and emission lines

Spectral lines arise from atoms or molecules undergoing transitions between two energy states differing in energy by ΔE . Such transitions in the hydrogen atom are shown as arrows in Fig. 10.1. If the atom is going from a high (excited) energy state to a lower energy state, the excess energy is emitted as a photon of energy $\Delta E = h\nu$. If many atoms do this, many photons with the same energy are emitted giving rise to an *emission line* (Fig. 1a), provided the photons can emerge without further scatters.

On the other hand, if these atoms are being excited to a higher energy state through the absorption of photons, only those photons of the correct energy, $\Delta E = h\nu$ will be absorbed. If the absorbing atoms are between us and the source of the original photons (say, a hot star), a deficiency of photons at that frequency, an *absorption line*, will be observed.

Each type of atom or molecule emits or absorbs radiation at frequencies characteristic of that atom; the observed frequencies therefore indicate the type of atom involved. The sodium doublet ($\lambda \sim 589 \text{ nm}$) is one example, and the $\text{H}\alpha$ line of hydrogen at $\lambda = 656.2 \text{ nm}$ is another.

The emission and absorption processes are a function not only of the kinds of atoms that are present but also of the conditions of temperature and pressure in which the atoms find themselves. For instance, the hotter stars do not show hydrogen absorption because the hydrogen is entirely ionized. Thus the conditions in the stellar atmosphere are directly indicated by the presence or absence of certain lines. See for example our discussion of the Saha equation in Section 9.4.

Origin of spectral lines

Figure 11 shows how the emission and absorption lines arise. A hot incandescent lamp emitting a continuum spectrum illuminates a cool cloud containing sodium (Na) atoms. Three observers analyze the light with a prism; each has a different perspective, and each sees a different spectrum. Each can choose to observe the light emerging from the prism directly by eye (observers A,B) or with the aid of a lens and piece of film (observer C).

Observer A studies the light coming directly from the lamp and sees the continuum spectrum. Observer B studies the light from the cloud and observes the Na doublet in emission. The emission-line spectrum arises from the re-emission of the radiation initially absorbed by the Na atoms. If the gas is sufficiently hot, collisions of the gas atoms will also excite the atoms to produce the lines of interest;